Journal of Engineering and Technology for Industrial Applications

ITEGAM-JETIA

Manaus, v.12 n.58, p.908-919. March/April, 2026.
DOI: https://doi.org/10.5935/jetia.v12i58.3193

ISSN ONLINE: 2447-0228

RESEARCH ARTICLE OPEN ACCESS

ANALYTICAL AND NUMERICAL ANALYSIS OF STRESS CONCENTRATION SINGULARITIES IN PERFORATED COMPOSITE WING RIBS

Ishak Berkane[1], Zohra Labed[2]

[1,2]University of Brothers Mentouri Constantine 1, Mechanics Laboratory, Department of Mechanical Engineering, Faculty of Technology, Campus Chaab Erssas, Constantine, Algeria.

[1]https://orcid.org/0009-0001-2507-786X, [2]http://orcid.org/0009-0002-2454-585X

Email: ishak.berkane@doc.umc.edu.dz, zohra_labed@yahoo.fr

ARTICLE INFO

Article History
Received: December 24, 2025
Reviewed: January 26, 2026
Accepted: March 10, 2026
Published: April 30, 2026

Keywords:
Stress Concentration Factor (SCF),
Orthotropic Plates,
Finite Elements (Abaqus),
Fiber Orientation Angle,
Matlab.

ABSTRACT

Aeronautical structures commonly use perforated skin panels and wing ribs to reduce weight while maintaining satisfactory mechanical performance. However, the combined influence of aperture size, material anisotropy, and fiber orientation on global and net stress concentration factors in orthotropic composites remains insufficiently quantified. This work aims to analyze the stress concentration behavior of perforated panels made of isotropic and orthotropic composites. A uniaxial tensile load is modeled using the finite element method (Abaqus) and classical analytical models (Heywood, Lekhnitskii, and Green-Zerna), supplemented by parametric calculations in MATLAB for glass/epoxy and carbon/epoxy plates. The results show a maximum stress concentration factor of $K_{tg} \approx 6.6$ for a geometric ratio d/W = 0.5 under an applied stress of 10 MPa, with a maximum error of 5% between the analytical and numerical models. A reduction of approximately 60% in the concentration factor is observed for a fiber orientation of 0°. Finally, the study proposes global and local stress concentration maps that incorporate fiber geometry/orientation compatibility limits, enabling the optimization of composite wing ribs while preserving the advantages of lightness, stiffness, and control of local stress amplifications, and opening up prospects for the study of damage and fatigue.

I. INTRODUCTION

During their operational life, aircraft are mainly made up of thin metal or composite structures designed to withstand fundamental structural loads (tension, compression, and shear) as well as aerodynamic stresses. In order to maintain aerodynamic performance, it is essential that the chord geometry and wing profile are maintained with minimal elastic and plastic deformation. Wing ribs are essential internal structural components that support the wing surface, maintain the aerodynamic profile configuration, and transfer internal stresses. They play a key role in distributing and readjusting shear forces, which helps to reduce the effective span of the spars and reinforce the overall rigidity of the structure. In the 21st century, the use of metal and composite ribs has become essential due to their ability to improve mechanical properties, reduce structural weight, and enhance corrosion resistance.

Materials such as aluminum, steel, titanium, and their alloys are frequently used, along with an increasing proportion of sophisticated composite materials. In the aerospace, marine, and automotive industries, it is common to use panels and shells with various cutouts for functionality and weight reduction purposes. However, these geometric discontinuities such as holes, notches, or abrupt changes in cross-section represent potential points where stresses can concentrate, leading to cracking and premature failure. In reality, virtually all aeronautical structures have such geometric irregularities or microstructural anomalies, making it essential to examine in detail their impact on the strength and longevity of structures. Much previous work has been devoted to modeling and analyzing the stress concentrations induced by these discontinuities.

By [1] used the finite element method in Abaqus to study the stress fields in ribs pierced with circular, elliptical, and rectangular cutouts, showing that optimizing the geometry of the openings improved the mechanical strength of light aircraft ribs. Similarly [2] analyzed the behavior of composite ribs subjected to different types of loading and fiber orientations using numerical tools, evaluating the stress tensor and critical displacements. Furthermore, classical analytical work carried out by [3-7] has provided reference solutions for stress concentration in perforated isotropic plates, particularly in the presence of circular holes. More recently, several studies have examined the influence of the diameter/width ratio, the stress concentration factor (SCF), and deformations in isotropic and orthotropic plates subjected to static tensile and shear stresses [8-10].

In this context, the present work takes a comparative approach to the mechanical behavior of perforated rectangular plates, representative of wing ribs with and without circular cutouts. The finite element technique is used to determine the stress concentration factors around a central circular hole in isotropic and orthotropic plates exposed to a unidirectional tensile load. The key parameters examined include the diameter/width ratio d/W, the fiber direction, and the length/width geometric proportions. Various materials are involved in the numerical simulations performed in Abaqus: Al 2024-T3 aluminum, glass/epoxy composite, and carbon/epoxy composite. The primary goal of this research is to examine and compare the global and net stress concentration factors in isotropic and composite plates with holes, in order to deepen our understanding of the combined effect of the geometry of the openings and the direction of the fibers. To this end, the following research questions are posed:

- RQ1: How does the d/W ratio influence the global and net stress concentration factors in isotropic and composite plates?
- RQ2: To what extent does fiber orientation modify the intensity and distribution of stresses around a circular hole?
- RQ3: What is the level of agreement between analytical predictions and results obtained using the finite element method for different geometric and material configurations?

This work makes several original contributions. First, it provides an in-depth parametric analysis of global and net stress concentration factors as a function of the d/W ratio, fiber orientation, and material type (Al 2024-T3, glass/epoxy, and carbon/epoxy). Second, it implements cross-validation between numerical simulations in Abaqus and analytical calculations implemented in MATLAB, making it possible to identify the areas of validity and limitations of simplified analytical models. Third, it highlights the particular effect of fiber alignment on stress concentration in composite wing ribs, including for configurations with multiple openings. Finally, the numerical results are verified using analytical calculations performed in MATLAB, ensuring the overall consistency of the various methods while highlighting the limitations of analytical models in certain complex configurations. This research is distinguished by its in-depth examination of the impact of fiber alignment on stress density in composite wing ribs, specifically with regard to plates with two circular holes. It thus contributes to improving the structural behavior of aeronautical composite structures.

II. MATERIALS, METHODS, AND THEORETICAL MODELING

In this study, there are two complementary steps involved in examining the mechanical behavior of wing structures and the problem of stress concentrations. First, using a profile of NACA-2414 to model and simulate an aircraft wing, with or without skin, depending on whether the ribs are cut out or not. By using the finite element method, it is possible to model and simulate the distribution of stresses at the ribs and wing section. Pre-processing includes generating the geometric model imported from a Python program, extracting the geometry and mesh, assigning material properties, and defining boundary conditions and loads to determine stress intensities and concentrations. The second stage, which is theoretical in nature, involves analyzing the geometric discontinuities responsible for stress concentrations using orthotropic perforated rectangular test specimens (Glass/Epoxy and Carbon/Epoxy) measuring 100 × 50 × 1 mm, cut from the wing rib. These specimens were studied numerically using the finite element method in Abaqus [11] to evaluate the global and net stress concentration factors around the circular openings. The influence of fiber orientation $\theta=[0°,90°]et[0°,-90°]$ was examined using MATLAB [12] , as was the effect of the geometric ratio (d/W), which varies between 0.1 and 0.5, on the stress concentration factor values. The stress concentration factor (SCF) is defined, as stated by Peterson in 1974, as the ratio of the maximum local stress to the nominal applied stress: $\theta=[0°,90°]et[0°,-90°]$

$$K_t = \frac{\sigma_{max}}{\sigma_{nom}} \quad (1)$$

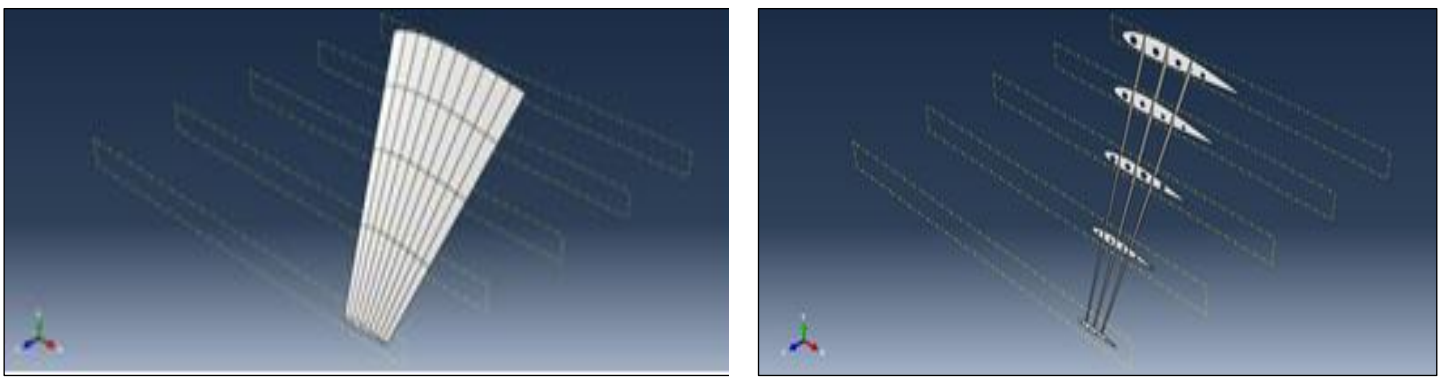

Figure 1: Aircraft wing with/without coating with hole.
Source: Authors, (2026).

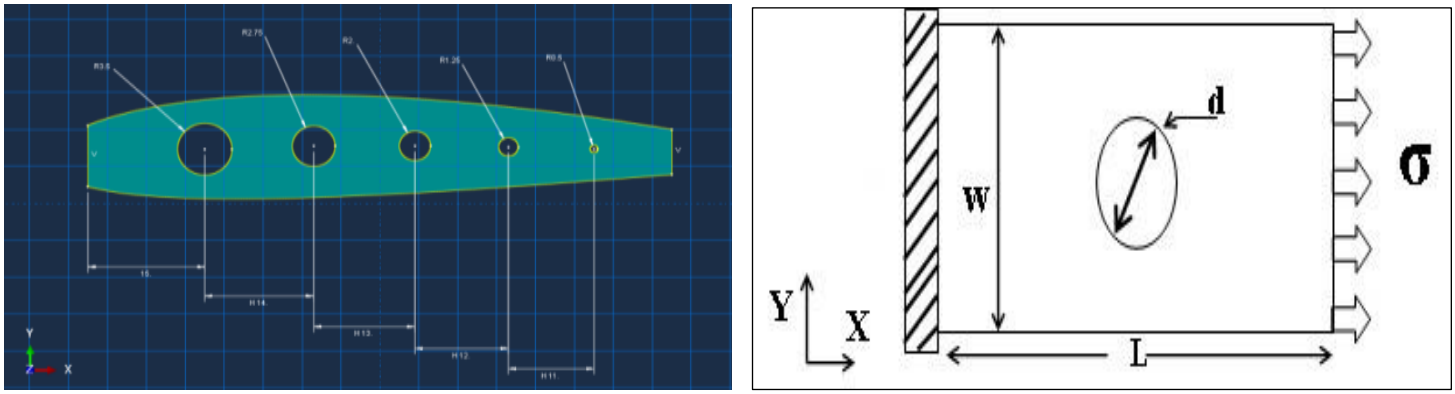

Figure 2: Plate with central hole subjected to uniaxial tension.
Source: Authors, (2026).

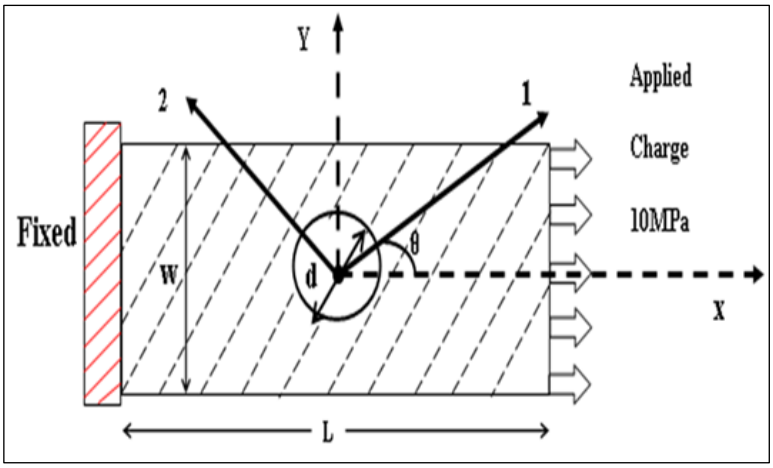

Figure 3: Laminated composite plate with circular hole.
Source: Authors, (2026).

For a rectangular orthotropic plate that has a central circular hole, Heywood (1952) proposed the following expression:

$$\frac{K_{Tg}^{\alpha}}{K_{tg}} = \frac{3\left(1-\frac{d}{w}\right)}{2+\left(1-\frac{d}{w}\right)^{3}} + \frac{1}{2}\left(\frac{d}{w}M\right)^{8}\left(K_{T}^{\alpha}-3\right)\left(1-\left(\frac{d}{w}M\right)^{3}\right) \quad (2)$$

Where K_{Tg}^{α} and K_{Tg} represent the stress concentration factors for an infinite and a finite plate, respectively. The magnification factor (M) is solely dependent on the geometric ratio (d/W).

$$M^{2} = \sqrt{1-8\left(\frac{3\left(1-\frac{d}{w}\right)}{2+\left(1-\frac{d}{w}\right)^{3}}-1\right)}\Big/2\left(\frac{d}{w}\right)^{2} \quad (3)$$

Lekhnitskii (1963) [13] introduced an alternative formulation of the SCF for orthotropic plates :

$$K_{T}^{\alpha} = 1+\sqrt{2\left(\left(\sqrt{\frac{E_{11}}{E_{22}}}\right)-\nu_{12}\right)+\frac{E_{11}}{G_{12}}} \quad (4)$$

Where:

E_{11} and E_{22} are the moduli of elasticity in the main directions.
G_{12} = is the in-plane shear modulus.
ν_{12} = is the Poisson's ratio.

An infinite SCF equal to 3 for an isotropic plate with a circular hole By simplifying the equation (2) we have:

$$\frac{K_{Tg}^{\alpha}}{K_{tg}} = \frac{3\left(1-\frac{d}{w}\right)}{2+\left(1-\frac{d}{w}\right)^{3}} \tag{5}$$

$$\sigma_{avg} = \frac{\sigma_{nom}}{1-\frac{d}{w}} \tag{6}$$

The SCF using Heywood's formulation will then be:

$$K_{Heywood} = K_{Tg}\left(1-\frac{d}{w}\right) \tag{7}$$

Lekhnitskii's (1963) theory is chosen to analyze the stress distribution in an orthotropic plate, the expression of the SCF corresponding to Lekhnitskii's theory is :

$$\begin{aligned} K_t = \frac{\sigma_\alpha}{\sigma^\infty} = \frac{E_\alpha}{E_1}\Big[-(\cos\varphi)^2 + (m+n)(\sin\varphi)^2\Big] m(\cos\alpha)^2 + \\ \Big[(1+n)(\cos\varphi)^2 - m(\sin\varphi)^2\Big](\sin\alpha)^2 - \\ n(1+m+n)\sin\varphi\cos\varphi\sin\alpha\cos\alpha \end{aligned} \tag{8}$$

Where:

E_α = modulus of elasticity in the direction defined by the angle α given by the following relationship :

$$\frac{E_\alpha}{E_1} = \frac{1}{(\sin\alpha)^4 + \frac{E_1}{E_2}(\cos\alpha)^4 + \frac{1}{4}\left(\frac{E_1}{G_{12}} - 2\nu_{12}\right)(\sin 2\alpha)^2} \tag{9}$$

φ = Angle of application of the tensile force relative to the main elastic axis.

α = Location angle of stress concentration factor.

The values of m and n are defined by :

$$m = \sqrt{\frac{E_x}{E_y}} \qquad n = \sqrt{2\left(\left(\sqrt{\frac{E_x}{E_y}}\right) - \nu_{xy}\right) + \frac{E_x}{G_{xy}}} \tag{10}$$

The elastic characteristics $\{E_x, E_y, G_{xy}, \nu_{xy}, \nu_{yx}\}$ in the reference frame (x, y) are linked to the material elasticity characteristics $\{E_1, E_2, G_{12}, \nu_{12}, \nu_{21}\}$ by equations: (13), (14), (15), (16):

$$\begin{aligned} \frac{1}{E_x} &= \frac{C^4}{E_1} + \frac{S^4}{E_2} + \left(\frac{1}{G_{12}} + \frac{2\nu_{21}}{E_1}\right)C^2S^2 \\ \frac{1}{E_y} &= \frac{S^4}{E_1} + \frac{C^4}{E_2} + \left(\frac{1}{G_{12}} + \frac{2\nu_{21}}{E_1}\right)C^2S^2 \\ \frac{\nu_{xy}}{E_y} &= \frac{\nu_{yx}}{E_x} = \frac{\nu_{21}}{E_1} - \left(\frac{1}{E_1} + \frac{1}{E_2} + \frac{2\nu_{21}}{E_1} - \frac{1}{G_{12}}\right)C^2S^2 \\ \frac{1}{G_{xy}} &= \left(\frac{1}{E_1} + \frac{1}{E_2} + \frac{2\nu_{21}}{E_1}\right)C^2S^2 + \frac{1}{G_{12}}\left(C^2+S^2\right)^2 \end{aligned} \tag{11}$$

In equations (13), (14), (15) and (16), the parameters C and S are the cosine and sine of the angle between the fibers and the x-axis. To determine the stress distribution around the circular hole in a composite plate. According to the theory of Green and Zerna (1654) [14] , the FCC can be expressed by the following formula:

$$K_t = \frac{\sigma_\alpha}{\sigma^\infty} = \frac{N_1 + N_2 + N_3}{\left(1+\gamma_1^2 - 2\gamma_1\cos 2(\alpha-\theta)\right)\left(1+\gamma_2^2 - 2\gamma_2\cos 2(\alpha-\theta)\right)} \tag{12}$$

The expressions for γ_1 and γ_2 are :

$$\gamma_1 = \frac{\sqrt{\left(\frac{E_2}{2G_{12}} - \gamma_{21} + \sqrt{\left[\left(\frac{E_2}{2G_{12}} - \gamma_{21}\right)^2 - \frac{E_2}{E_1}\right]}\right)} - 1}{\sqrt{\left(\frac{E_2}{2G_{12}} - \gamma_{21} + \sqrt{\left[\left(\frac{E_2}{2G_{12}} - \gamma_{21}\right)^2 - \frac{E_2}{E_1}\right]}\right)} + 1}$$

$$\gamma_2 = \frac{\sqrt{\left(\frac{E_2}{2G_{12}} - \gamma_{21} - \sqrt{\left[\left(\frac{E_2}{2G_{12}} - \gamma_{21}\right)^2 - \frac{E_2}{E_1}\right]}\right)} - 1}{\sqrt{\left(\frac{E_2}{2G_{12}} - \gamma_{21} - \sqrt{\left[\left(\frac{E_2}{2G_{12}} - \gamma_{21}\right)^2 - \frac{E_2}{E_1}\right]}\right)} + 1} \tag{13}$$

$$\begin{cases} N_1 = (1+\gamma_1)(1+\gamma_2)\left(1+\gamma_1+\gamma_2+\gamma_1\gamma_2 - \cos(\alpha-\theta)\right) \\ N_2 = -4\left[\gamma_1+\gamma_2-(1+\gamma_1\gamma_2)\cos 2(\alpha-\theta)(\sin\alpha)^2\right] \\ N_1 = -4(\gamma_1\gamma_2-1)\sin 2(\alpha-\theta)\sin\alpha\cos\alpha \end{cases} \tag{14}$$

Table 1: Results of mesh refinement.

Hole	Global stress concentration factor (analytic)	Global stress concentration factor (FEM)	
d/w	Heywood	Element Shape	Triangular
		Elements Number	Mesh type : STRI65
d/w=0.04	6.57	1134	4.296
	6.57	1341	5.159
	6.57	1461	5.298
	6.57	1572	6.915
	6.57	1632	6.080
	6.57	1676	6.099
	6.57	1711	6.166
	6.57	1728	6.351
	6.57	1742	6.599

Source: Authors, (2026).

To minimize computational costs, a coarse mesh was modeled in the region far from the critical areas, while local mesh refinement was conducted in the region around the openings. The triangular mesh used in the present analysis, consisting of STRI65 elements with six nodes, was shown to be efficient in the region with large stress concentrations. To validate the accuracy of the FEM simulation in the commercial code Abaqus, the mesh convergence study was conducted using the diameter-to-width ratio of d/W = 0.04 and comparing FEM data with Heywood's exact solution. It can be concluded that, using a coarse mesh with a smaller number of elements (total of 1134), the global stress concentration factor (K_t = 4.296) was lower than its exact value (K_t = 6.57), implying an error in the underestimation of stresses attributable to inadequate modeling of the stress gradient in the vicinity of the hole.

As the mesh was successively refined, the stress concentration factor gradually increased to 6.599 with a total of 1742 elements, being in excellent agreement with the exact results. This simulation results in excellent convergence of the FEM solution, thereby ascertaining the effectiveness of the triangular mesh in simulating accurately the localized stress pattern. The adopted strategy in mesh generation, thus, has proved to be most optimum in terms of computational accuracy and costs.

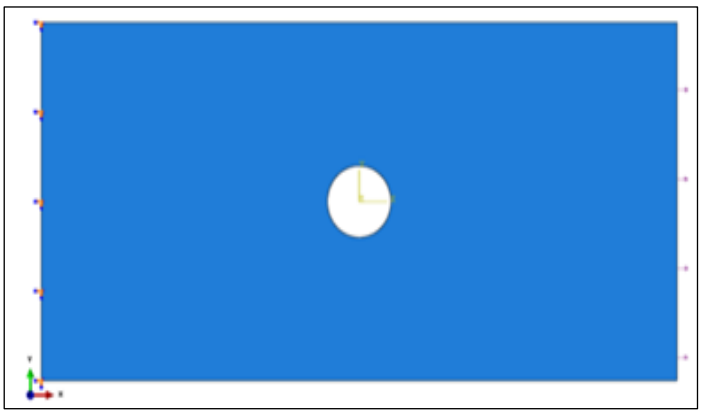

Figure 4a: Plate with central hole subjected to uniaxial tension.
Source: Authors, (2026).

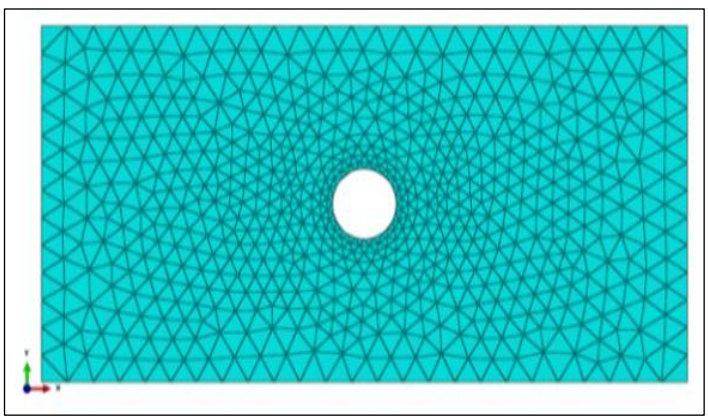

Figure 4b: Exemple typique de maillage et Conditions aux limites.
Source: Authors, (2026).

Table 2: Mechanical properties.

Material Parametres	Glass/Epoxy	Carbon/Epoxy
E_{11} (MPa)	50000	134000
E_{22} (MPa)	14500	10300
γ_{12} (MPa)	0,33	0,33
G_{12} (MPa)	2560	5500
G_{12} (MPa)	2560	5500
G_{22} (MPa)	2240	3200

Source: [15].

III. RESULTS AND DISCUSSIONS

III.1 STRESS VARIATION AND FIBER ORIENTATION IN THE DIRECTION OF TENSILE LOADING

Composite plates with a circular hole were subjected to tensile loading. The graphs show the variation of the stress concentration factor in the direction of uni-axial loading of the orthotropic plate fitted with circular hole of diameter (10, 16 , 22, 28, 30, 34).The different curves correspond to different fiber orientations θ (- 90°,- 60°,- 45, 0°,45°, 60°, 90°). The elastic characteristics of orthotropic materials given in table.

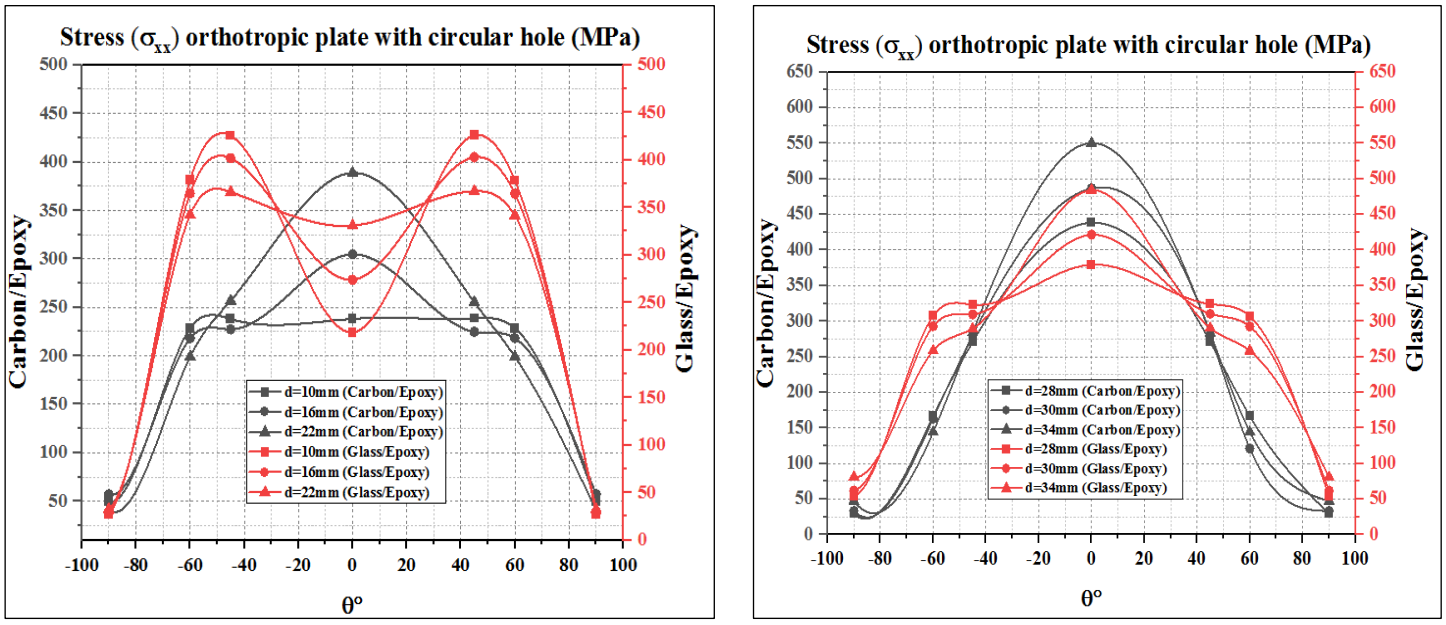

(a) (b)

Figure 5: variation in stress at edge of circular hole for (a) carbon/epoxy and (b) glass/epoxy.
Source: Authors, (2026).

The graph of a1 shows the variation in normal stress σ_{xx} as a function of the angle θ for orthotropic perforated plates (circular hole) made of composite materials of Carbon / Epoxy and Glass / Epoxy with three hole diameters of 10 mm, 16 mm, and 22 mm. It may be seen that, for both materials, the value of stresses attains a peak at around ± 45°. This indicates a critical zone of stress concentration generally associated with the effects of the hole's edge. Globally, for the same diameter, the levels of stresses in the Glass / Epoxy plates are greater than those in the Carbon / Epoxy plates, reflecting a lower capability to distribute charges around the discontinuity. Moreover, with the increase in diameter, there is a significant rise in maximum stress, particularly for the material Verre/Époxy.

This trend accentuates the greater sensitivity of this material to opening size, hence a susceptibility to strain concentration effects. On the other hand, the Carbon/Époxy plate shows a less abrupt increase in stresses with the increase of diameter, showing better ability to bear geometrical discontinuity. Finally, the symmetry of the curves with respect to the vertical axis (θ = 0°) translates to a symmetrical behavior of the stress distribution around the hole, which is typical of homogeneous loading of an orthotropic plate. These results highlight the importance of correctly choosing the material and the geometry of cutouts during the design stage, when composite structures are subjected to complex mechanical loading conditions.

Graph (b1) presents the normal stresses distribution, σ_{xx}, within an orthotropic plate with a circular hole as a function of the angle, θ, corresponding to three hole diameters, namely 28 mm, 30 mm, and 34 mm for two types of composite materials: Carbon/Epoxy and Glass/Epoxy. It can be noticed that for each curve, the maximum value appears at θ=0°, which indicates the loading direction; after that, these values decrease symmetrically towards ±90°. In addition, for the same diameter, the maximum stress value registered in carbon/epoxy material is far greater than that in the glass/epoxy ones, which implies higher rigidity.

Furthermore, increasing the hole diameter causes a significant rise in the maximum stress, which is due to the increasing concentration of loads around the opening. Hence, such a trend reflects the coupled effect of material and geometry on the distribution of stresses, a factor that plays a crucial role in the optimization of holed composite structures.

III.2 NUMERICAL SIMULATION AND ANALYTICAL EVALUATION OF STRESS CONCENTRATION IN ORTHOTROPIC PLATES

A study was conducted on a single-layer orthotropic plate with rectangular stratification of the same size as in the previous case and subjected to a uniform tensile load of 10 MPa. The global and net stress concentration factors were calculated using Heywood's analytical formulation based on equations and and were then compared with the data obtained using finite elements.

The comparative analysis shows good agreement between the two approaches, confirming the reliability of Heywood's formulation for estimating stress concentrations in an orthotropic plate.

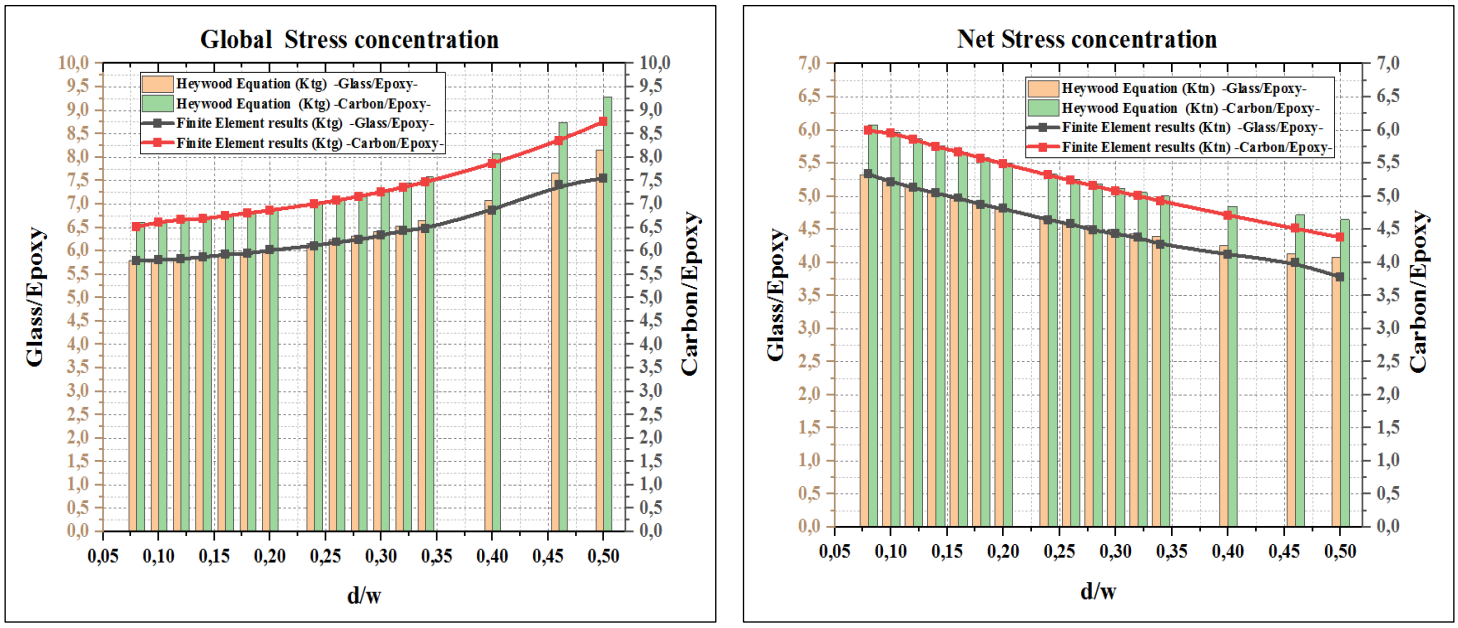

Figure 6: Comparison of stress concentration factors (Ktg and Ktn) for glass/epoxy and carbon/epoxy composites as a function of the ratio (d/w).
Source: Authors, (2026).

The above outcomes shown graphically reveal the development of global and net stress concentration factors with increasing values of (d/w), according to Heywood's analytical models and FEM computations, for flat orthotropic glass/epoxy and carbon/epoxy composite plates with holes. In general, the global stress concentration factor (K_{tg}) is observed to increase continuously with (d/w), while the net stress concentration factor (K_{tn}) is observed to decrease with the values of (d/w), due to the corresponding decrease in the cross-sectional area, with higher values registered by carbon/epoxy composites compared to glass/epoxy composites, reflecting higher stress sensitivity due to the presence of holes.

The present results show that there is an excellent fit between the values predicted by the analytical models and FEM computations, except slightly at higher values of (d/w), which can be better evaluated by the FEM method due to local stress adjustments around the hole that cannot be predicted by analytical models. These above outcomes show that, although the analytical models proposed by Heywood still provide useful estimates for moderate values, there is a need for FEM analysis, especially when dealing with extreme values of (d/w), and the difference between glass/epoxy and carbon/epoxy is due to the unique elastic properties of these composites.

III.3 ANALYSIS OF THE INFLUENCE OF THE FIBER ORIENTATION ANGLE θ° ON STRESS CONCENTRATION

Dans le cadre de l'étude de l'influence de la géométrie sur les facteurs de concentration des contraintes dans des stratifiés orthotropes, les équations constitutives (2) à (5) ont été implémentées sous MATLAB afin de calculer les facteurs de concentration globaux (K_{tg}) et nets (K_{tn}) en fonction du rapport entre le diamètre du trou circulaire et la largeur du stratifié (d/W). Les figures 19 et 20 présentent l'évolution de ces paramètres pour des stratifiés verre/époxy et carbone/époxy percés d'un trou circulaire, et ce pour différents rapports (d/W). Les facteurs de concentration (K_t) ont été déterminés pour plusieurs orientations de fibres (30°,45°,60°et 90°), à partir des équations analytiques sous MATLAB et des simulations numériques réalisées par éléments finis à l'aide du logiciel Abaqus.

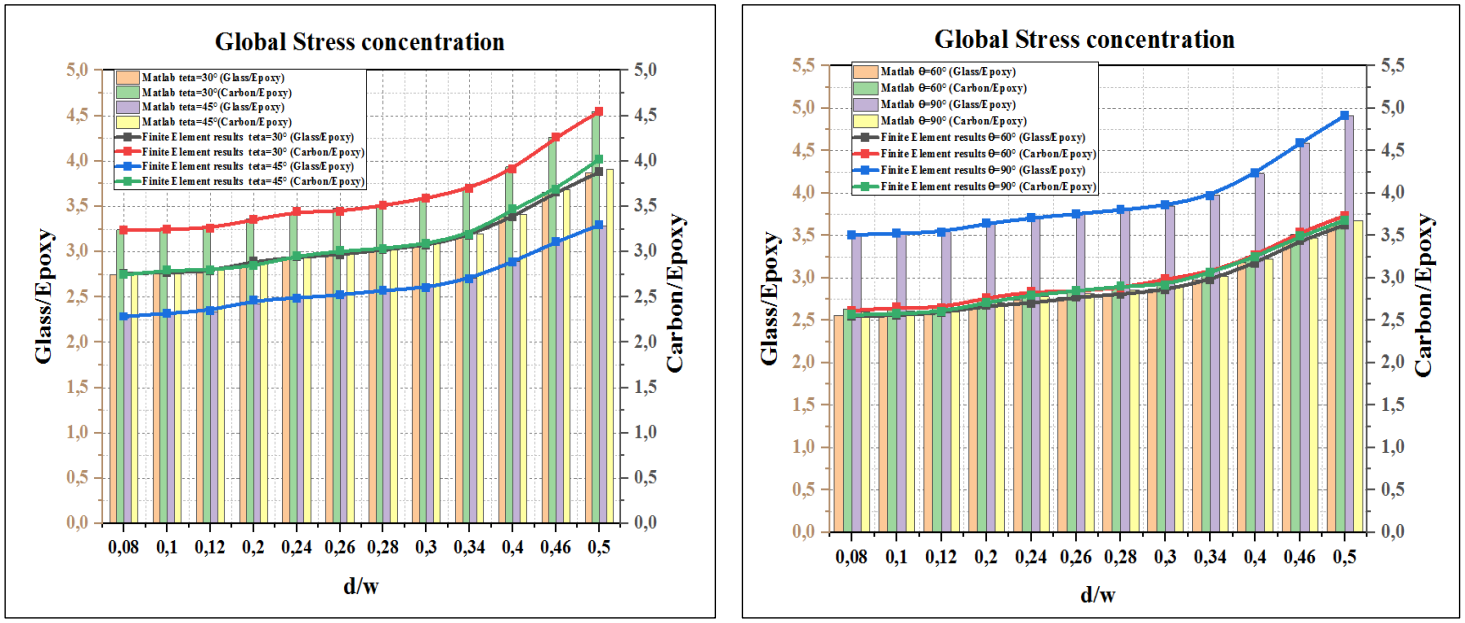

Figure 7: Evolution of the stress concentration factor K_{tg} for different fiber orientation angles (30°, 45°, 60°, 90°).
Source: Authors, (2026).

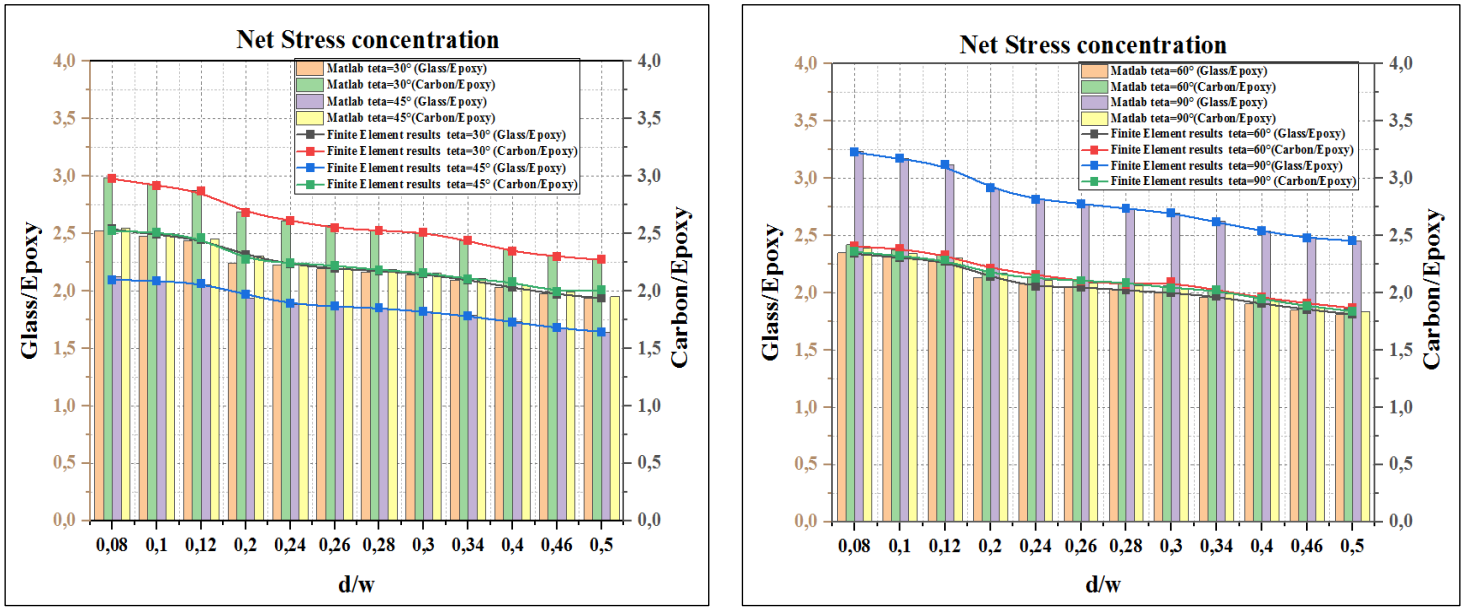

Figure 8: Evolution of the stress concentration factor K_{tn} for different fiber orientation angles (30°, 45°, 60°, 90°).
Source: Authors, (2026).

The deformations of stress concentration factors relative to the geometric ratio are presented for the four figures, regardless of their gross or total trend. These techniques are applied to glass/epoxy and carbon/epoxy composite laminates, viewed at various degrees in the fiber orientation space. The analytical findings solved using MATLAB are presented for the sake of clarity and are compared with their debatable numerical versions developed by finite elements. The results show that the net concentration factor follows a downward trend as the scale distributor competition in d/w increases, implying a more uniform redistribution of stresses as the relative aperture increases. On the other hand, the overall concentration factor increases sharply in proportion to for each value, reflecting an increase in local stiffness and stress amplification effects. In addition, the values for glass/epoxy composites are generally smaller than those for carbon/epoxy composites, indicating that glass/epoxy composites are less sensitive to stress concentration.

The discrepancy observed between analytical predictions and finite element results remains limited overall, but increases for high angles (θ =90°) and large ratios (d/w), reflecting the limitations of simplified analytical models in the face of local nonlinearities captured by numerical simulation. These observations confirm that fiber orientation and reinforcement type play a decisive role in controlling stress concentrations, and that hybrid modeling is necessary to reliably predict the mechanical behavior of laminated composites.

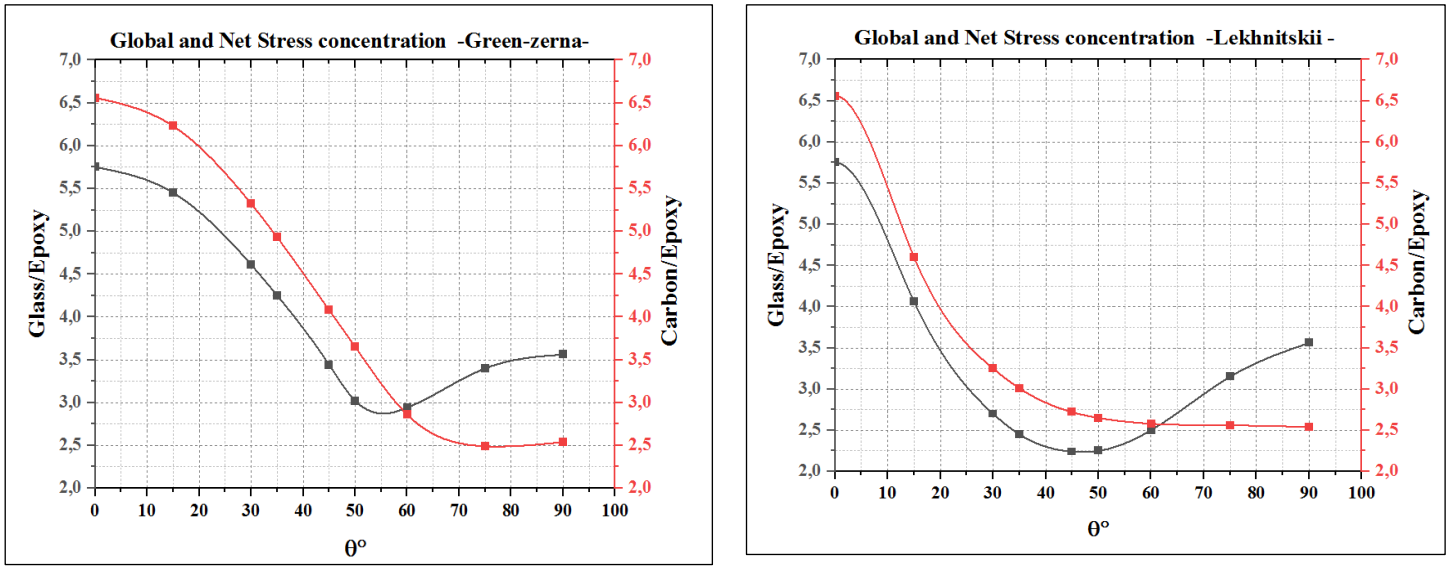

Figure 9: Influence of fiber angle θ on stress concentration for both theories: Glass/Epoxy and Carbon/Epoxy comparison.
Source: Authors, (2026).

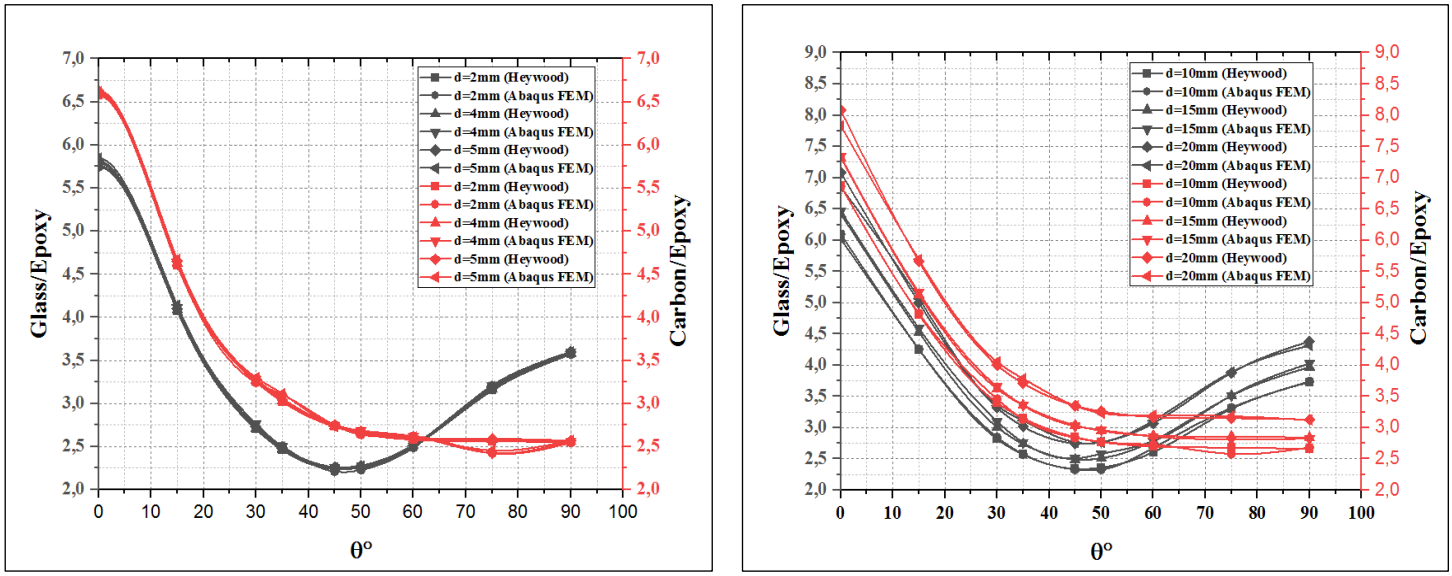

Figure 10: Variation of the stress concentration factor as a function of the inclination angle θ for Glass/Epoxy and Carbon/Epoxy materials as a function of the ratio (d).
Source: Authors, (2026).

The analytical and numerical results clearly demonstrate that fiber orientation, denoted as, has a dominant effect on stress concentrations around a hole in composite plates. As changes from 0° to 90°, there is a substantial reduction (about 60%) in stress concentrations, as measured by stress concentration factor K_t, because of a more efficient stress field with increasing deviation from loading in the fiber orientation direction. These results are observed for Glass/Epoxy and Carbon/Epoxy composite materials, for which lower Kt values are expected for Carbon/Epoxy, because of increased specific stiffness and efficient stress transfer from fibers to matrices. Variations in Kt with respect to different theoretical models (Green-Zerna, Lekhnitskii, Heywood) are dominated by coupling effects due to shear/extension and anisotropy, for which Green-Zerna models show a steeper non-linear variation, while for Lekhnitskii, a smoother variation is observed.

Also, hole diameters show a significant effect, for which larger holes at small orientations lead to higher K_t, while at small diameters, a more homogenous stress field with less orientation dependence is observed. Usually, a minimum for K_t is observed for orientations near (= 45°-60°), at which optimal mix of longitudinal and transverse stiffness is achieved. In practice, orientation of layers near 90° decreases stress overconcentration with potential reduction in plate stiffness, increasing susceptibility to shear damage. These observations, supported by a good fit of analytical results with FE data from Abaqus, establish that this modeling study, through non-linear analysis and validation, assesses optimal fiber orientation of layers around holes in composite laminates.

III.4 EFFECT OF FIBER ORIENTATION ON THE VALUES AND LOCATION OF THE STRESS CONCENTRATION FACTOR

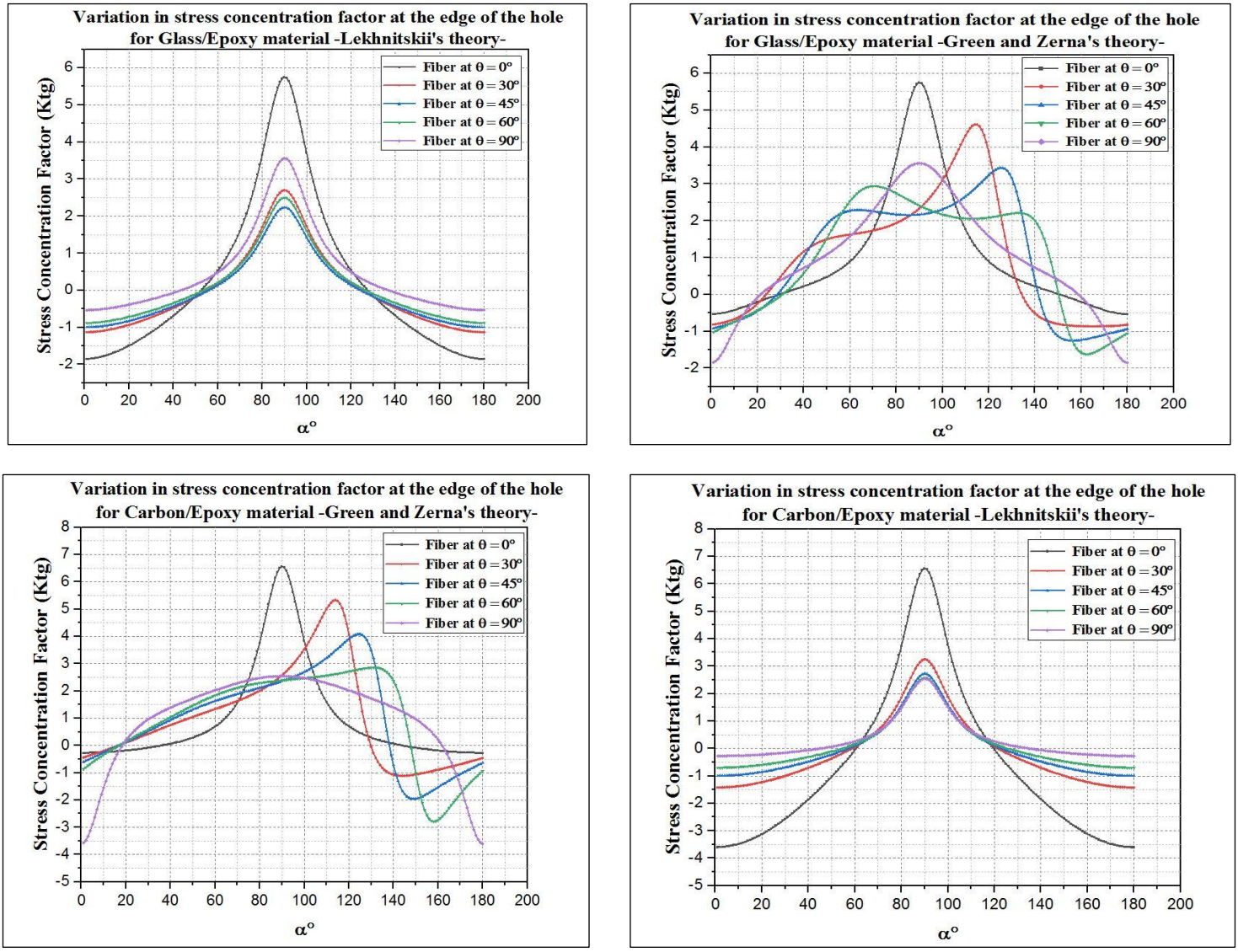

Figure 11: Influence of fiber orientation on the distribution of the stress concentration factor at the edge of a hole in a glass/epoxy and carbon/epoxy composite (Green and Zerna/Lekhnistskii theory).
Source: Authors, (2026).

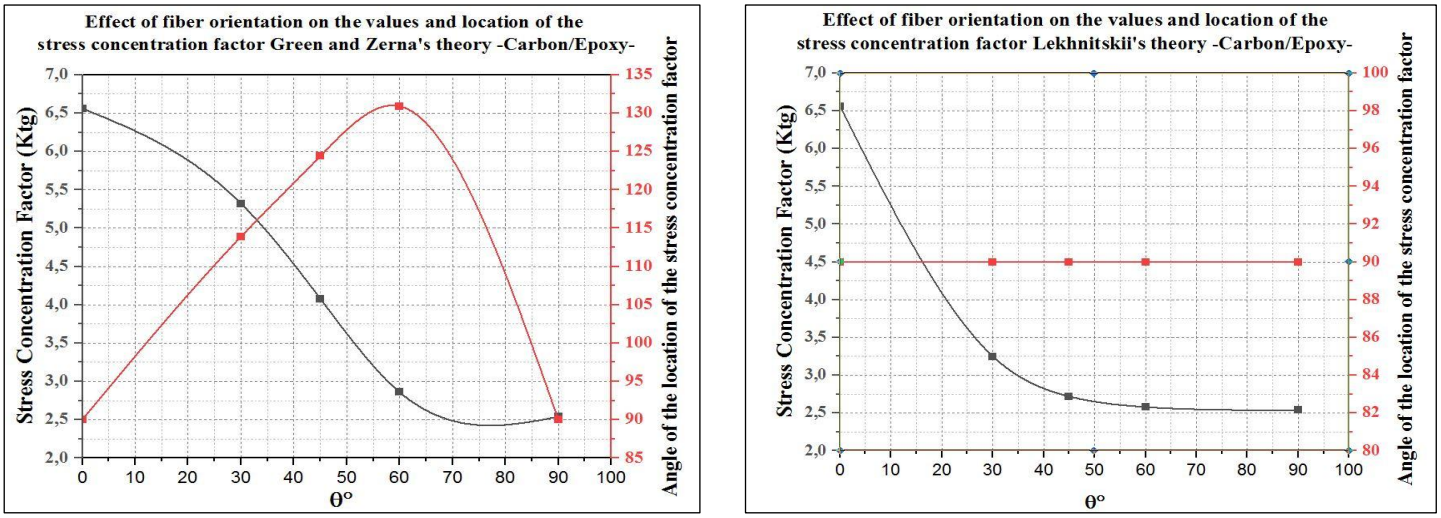

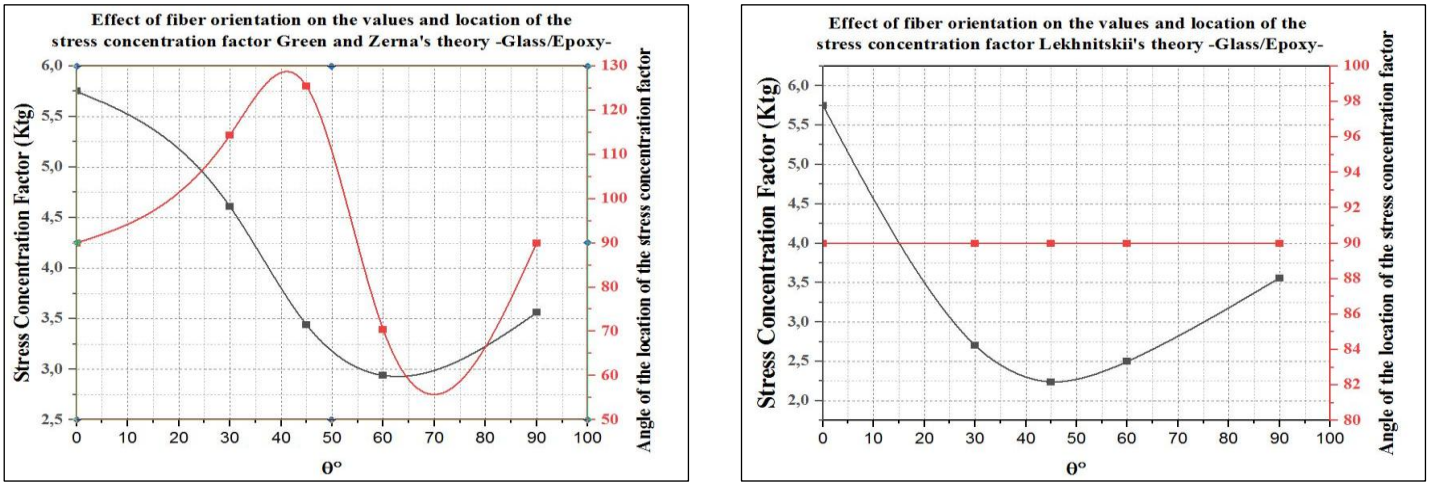

Figure 12: Effect of fiber orientation on the value and position of the stress concentration factor in glass/epoxy and carbon/epoxy composites (Green and Zerna/Lekhnistskii theory).
Source: Authors, (2026).

The figures clearly show the sensitivity of the fiber orientation, θ, to amplitude, as predicted by theory, at the central position of maximum stress around a hole. In both contexts, the stacking density, K_t, decreases sharply as the orientation approaches 90° while θ varies from 0° to a maximum of 90°, corresponding to 2.5, i.e., 60% attenuation. However, there are differences concerning the angle of location of the maximum; Green & Zerna predict a non-monotonic shift of this angle, which increases from θ = 0° to as far as 130° around θ = 50°-60°, finally returning to 90° as a function of θ, while it reaches 90°.

Lekhnitskii's solution has long attributed an almost constant angle of 90° to it. Expression: The angular variation predicted by Green & Zerna describes the anisotropic superposition in terms of shear fields and axial fields. On the other hand, in the method used by Lekhnitskii, critical localization does not take into account this transition of the stress field. In terms of practical prediction, it appears that the selection of material orientation not only reduces the level of critical stress localization (which is beneficial in terms of resistance to drilling and cracking), but can also cause it to vary.

IV.CONCLUSIONS

This research aimed at improving the comprehension and mathematical evaluation of the combined effect of opening geometry characteristics, material properties of elasticity, and orientation angles on stress concentration phenomena in isotropic and orthotropic plates resembling aircraft wings. By choosing a research approach that applies comprehensive mathematical modeling, numerical simulations using finite elements, and parametric calculations, many important results were obtained. It was found that the value of the general stress concentration factor K_{tg} systematically increased with the value of the geometric ratio d/W, thus expressing the effect of relative hole size on the local stress concentration. At a constant uniaxial stress of 10 MPa, the greatest value of $K_{tg} \approx 6.6$ was found at d/W = 0.5, in agreement with Heywood's classical mathematical calculations for thin perforated plates.

In fact, a mesh convergence test was performed in order to establish the validity of the finite-element numerical model, as differences between numerical and mathematical computations stayed below the limit of ±5% for representative hole sizes. Apart from geometric effects, other outcomes emphasized the importance of material anisotropy and orientation angles for composite plates. Both computational and analytical results clearly indicated that by varying the orientation angle from 0° to 90°, there is a remarkable decrease in the value of stress concentration factor, approximately 60% for glass/epoxy and carbon/epoxy materials. The minimum value for this concentration factor occurs for intermediate angles lying between 45° and 60° because of an optimized balance between longitudinal and transverse stiffness.

In general, materials with higher stiffness, such as carbon/epoxy, are expected to display higher values of stress concentration for given values of d/W comparison than glass/epoxy materials. Additionally, this comparison between global and net stress concentration factors highlighted interesting trends: K_{tg} is expected to increase with increasing values of d/W, but there is a concurrent decrease in K_{tn} because of the reduction in net cross-section. In fact, both parameters should be considered simultaneously for designing perforated structures. What makes these findings important is their direct relevance to the design and optimization of composite materials in the field of aerospace. These findings show that in managing stress concentrations in the vicinity of holes, effective design cannot be achieved in a purely geometrical manner, focusing solely on minimizing hole size, but that material selection and orientation also have to be carefully modeled.

The parametric maps obtained from this research activity can assist in design optimization, especially in wing ribs, where weight minimization has to be combined with limitations imposed by ultimate stresses that may cause material failure. In addition, their validation, obtained here relying on comparisons among Hood, Lekhnitskii, and Green-Zerna theories, Finite Element methods, confirms that the adoption of these models in the initial design phases makes sense but also that, in certain cases, Finite Element computations are required, namely when dealing with highly anisotropic materials. However, these results are to be viewed in consideration of the above-mentioned limitations. The analyses were carried out in the context of the linear-elastic model, static load, and the absence of phenomena of initial damage and progressive damage. The role of material nonlinearity, damage, delamination, and cyclic loads has not been accounted for, although they are crucial for the lifetime of the aerospace structure.

Therefore, further research needs to focus on the integration of the above-mentioned fields, such as progressive damage analysis, fatigue analysis, crack initiation around openings, and the validation of the results on perforated composite samples.

V. AUTHOR'S CONTRIBUTION

Conceptualization: Ishak Berkane and Zohra Labed.
Methodology: Ishak Berkane and Zohra Labed.
Investigation: Ishak Berkane.
Discussion of results: Ishak Berkane and Zohra Labed.
Writing – Original Draft: Ishak Berkane.
Writing – Review and Editing: Ishak Berkane and Zohra Labed.
Resources: Ishak Berkane and Zohra Labed.
Supervision: Zohra Labed.
Approval of the final text: Ishak Berkane and Zohra Labed.

VI. REFERENCES

[1] S. Bairavi, "Design And Stress Analysis of Aircraft Wing Rib With Various Cut Outs," vol. 358, no. 4, pp. 511–514, 2016.

[2] M. A. Bennaceur, Y. M. Xu, and H. Layachi, "Wing Rib Stress Analysis and Design Optimization Using Constrained Natural Element Method," *IOP Conf. Ser. Mater. Sci. Eng.*, vol. 234, no. 1, pp. 0–7, 2017, doi: 10.1088/1757-899X/234/1/012018.

[3] R. B. Heywood, "Photoelasticity for Designers," *Strain*, vol. 5, no. 4, pp. 238–238, 1969, doi: 10.1111/j.1475-1305.1969.tb01629.x.

[4]N. I. Muskhelishvili, *Some Basic Problems of the Mathematical Theory of Elasticity*. 1977. doi: 10.1007/978-94-017-3034-1.

[5] S.P. Timoshenko and J.N.Goodier, "Theory of Elasticity: S.P. Timoshenko, J.N. Goodier." 1934.

[6] R.C.J. Howland, (1930)., "On the stresses in the neighbourhood of a circular hole in a strip under tension," *Philos. Trans. R. Soc. London. Ser. A, Contain. Pap. a Math. or Phys. Character*, vol. 229, no. 670–680, pp. 49–86, 1930, doi: 10.1098/rsta.1930.0002.

[7] W. D. Pilkey and D. F. Pilkey, *Peterson's stress concentration factors*, vol. 35, no. 06. 2013. doi: 10.5860/choice.35-3328.

[8] N. K. Jain and N. D. Mittal, "Finite element analysis for stress concentration and deflection in isotropic, orthotropic and laminated composite plates with central circular hole under transverse static loading," *Mater. Sci. Eng. A*, vol. 498, no. 1–2, pp. 115–124, 2008, doi: 10.1016/j.msea.2008.04.078.

[9] M. Mohammadi, J. R. Dryden, and L. Jiang, "Stress concentration around a hole in a radially inhomogeneous plate," *Int. J. Solids Struct.*, vol. 48, no. 3–4, pp. 483–491, 2011, doi: 10.1016/j.ijsolstr.2010.10.013.

[10] S. Deghboudj, H. Satha, and W. Boukhedena, "Effect of shape factor upon stress concentration factor in isotropic/orthotropic plates with central hole subjected to tension load," *UPB Sci. Bull. Ser. D Mech. Eng.*, vol. 78, no. 4, pp. 143–154, 2016.

[11] Dassault Systèmes, *ABAQUS User's Manual*, Version 6.13, Providence, RI, USA, 2013.

[12] MathWorks, *MATLAB User's Guide*, Release R2015a, Natick, MA, USA, 2015.

[13]"S G Lekhnitskii-Anisotropic plates-Gordon and Breach Science Publishers (1984)."

[14] A. E. Green and W. Zerna, "Theoretical Elasticity," *Physics Today*, vol. 23, no. 5. pp. 71–73, 1970. doi: 10.1063/1.3022126

[15] D. Samir, B. Wafia, and S. Hamid, "Analyse numérique de la concentration de contraintes dans une plaque composite sollicitée en traction comportant deux trous," Rev. des Compos. des Mater. Av., vol. 26, no. 2, pp. 147–163, 2016, doi: 10.3166/rcma.26.147-163.